Polarimetry of Polarized Positrons

K. Peter Schuler

R&D polarimetry at or near source energies (5-50 MeV)

- **Low-Energy Positron Polarimetry**
  - **general choices and considerations**
- **Basics of the Transmission Method**
  - **for photon polarimetry**
  - **for positron polarimetry**
- **Positron Polarimetry at E166**
  - **photon polarimeter**
  - **positron polarimeter**
- **Expected Performance and Preliminary Results**

high-energy Compton polarimetry at ILC energies (45.6-500 GeV)

- **only some brief remarks**

Spin-Dependent Processes at Low Energy

- $e^+X \rightarrow e^+X$ — **Mott scattering**
- $e^+e^- \rightarrow e^+e^-$ — **Bhabha scattering**
- $e^+e^- \rightarrow (e^+e^-)^* \rightarrow \gamma\gamma$ — **positronium formation & decay**
- $e^+e^- \rightarrow \gamma\gamma$ — **annihilation in flight**
- $\gamma e^+ \rightarrow \gamma e^+$ — **Compton laser backscattering**
- $e^+X \rightarrow \gamma X$ **brems.)** — $e^+ \rightarrow \gamma$ **reconversion and subsequent** $\gamma e^- \rightarrow \gamma e^-$
- $e^+e^- \rightarrow \gamma\gamma$ **annih.)** — **Compton scattering on pol.** e^- **in 2-step process**

- **both collision partners need to be polarized, except for Mott scattering (spin-orbit effect), positronium polarimetry (magn. field) and bremsstr.**
- **primary interest is in longitudinal source polarization and polarimetry**
- **Mott polarimetry requires spin rotator (transverse spin effect)**
- **viability and technique for polarimetry depends greatly on**
  - the analzing power of the physical process
  - source intensity, time structure, emittance
  - beam energy

Low-Energy Positron Polarimetry

candidate processes considered for E166

- **Photons: Compton Scattering on polarized electrons**
  - **forward scattering** (e.g. Schopper et al.)
  - **backward scattering**
  - **transmission method** (e.g. Goldhaber et al.)
- **Positrons: all on ferromagnetic = polarized e^- targets**
  - **Annihilation polarimetry ($e^+e^- \rightarrow \gamma\gamma$)** (e.g. Corriveau et al.)
  - **Bhabha scattering ($e^+e^- \rightarrow e^+e^-$)** (e.g. Ullmann et al.)
  - **brems/annihilation ($e^+ \rightarrow \gamma$)** plus **γ-transmission (Compton) polarimetry**

principle difficulties of e^+ polarimetry:

- **huge multiple-scattering at low energies even in thin targets**
- **cannot employ double-arm coincidence techniques**
  or single-event counting due to poor machine duty cycle (bunch length ~ ps)
- **low energies below 10 MeV, very vulnerable to backgrounds**

conclusion from studies for ATF and E166:

$\Rightarrow$ **the transmission method is the most suitable method for low-energy positron polarimetry for linear collider type polarized positron sources**

Transmission Polarimetry of (monochromatic) Photons

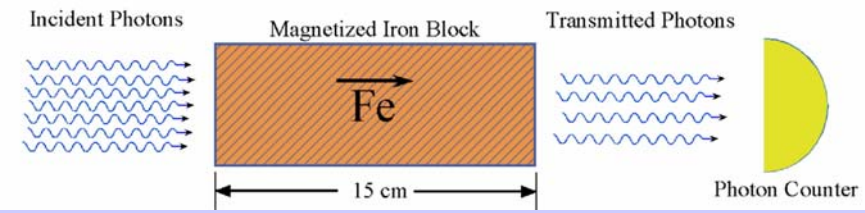

M. Goldhaber et al.
Phys. Rev. 106 (1957) 826.

$$\sigma = \sigma_{phot} + \sigma_{comp} + \sigma_{pair}$$

$$\sigma_{comp} = \sigma_0 + P_\gamma P_e \sigma_P$$

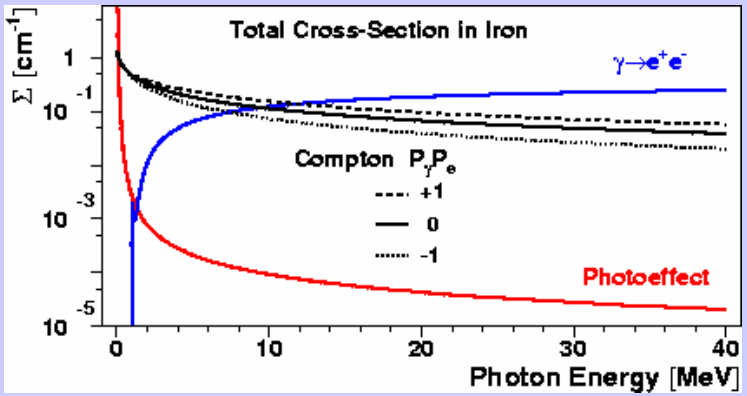

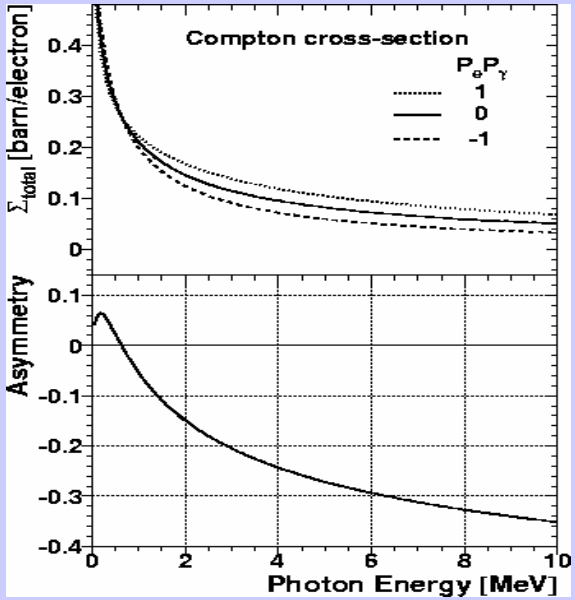

$$T^{\pm}(L) = e^{-nL\sigma} = e^{-nL(\sigma_0+\sigma_{phot}+\sigma_{pair})}\, e^{\pm nLP_eP_\gamma\sigma_P}$$

$$\delta(L) = \frac{T^+(L) - T^-(L)}{T^+(L) + T^-(L)} = \tanh(nLP_eP_\gamma\sigma_P) \approx nLP_eP_\gamma\sigma_P$$

all unpolarized contributions cancel in the transmission asymmetry δ (monochromatic case)

Transmission Polarimetry of Photons

monochromatic case

$$P_\gamma = \frac{\delta}{P_e A_\gamma}$$

Analyzing Power:

$$A_\gamma(L) \equiv \frac{\delta(L)}{P_e P_\gamma} \approx nL\sigma_P$$

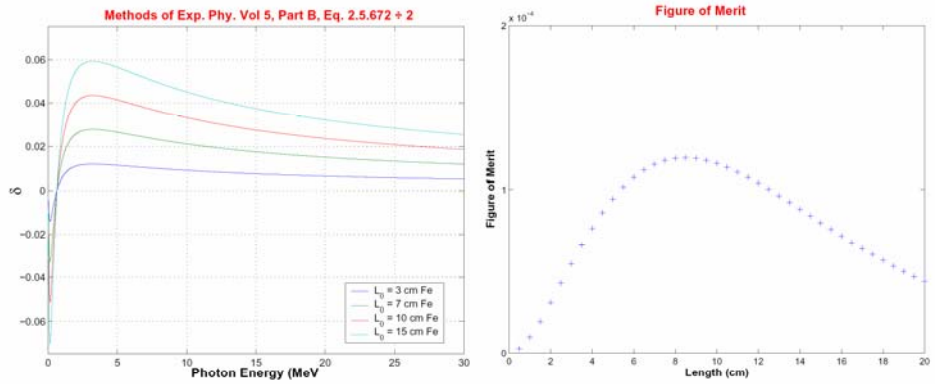

Figure 15: (**a**) The asymmetry δ defined in eq. (15) for transmission polarimetry of MeV photons in various lengths of iron. (**b**) The figure of merit $A_\gamma^2 T$ for 7.5 MeV photons as a function of the length of a transmission iron polarimeter

photon spectra from undulator- or Compton-based photon sources are not at all monochromatic: must use integrated numbers or energies:

non-monochromatic case

$$N_{+(-)} = \int_{\omega_0^{min}}^{\omega_0^{max}} \frac{dN_{+(-)}}{d\omega_0}(\omega_0)d\omega_0,$$

$$E_{+(-)} = \int_0^{\omega_0^{max}} \omega_0 \frac{dN_{+(-)}}{d\omega_0}(\omega_0)d\omega_0,$$

$$\delta = \frac{N_+ - N_-}{N_+ + N_-} = P_e \langle P_\gamma \rangle \langle A_\gamma \rangle$$

$$\delta^E = \frac{E_+ - E_-}{E_+ + E_-} = P_e \langle P_\gamma^E \rangle \langle A_\gamma^E \rangle$$

Transmission Polarimetry of Positrons

2-step process:

- **re-convert e+ → γ via brems/annihilation process**
  - **polarization transfer from e+ to γ proceeds in a well-known manner**
- **measure polarization of re-converted photons with the photon transmission method discussed earlier**
  - **infer the polarization of the parent positrons from the measured photon polarization**

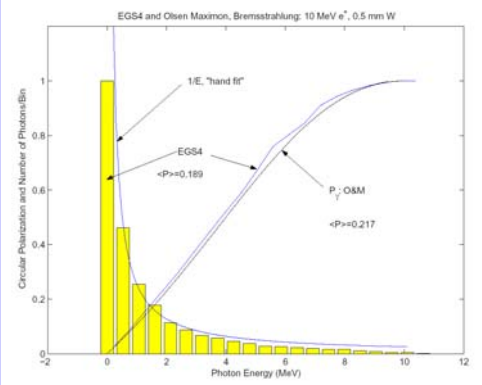

Fronsdahl & Überall;
Olson & Maximon;
Page; McMaster

experimental challenges:

- **huge angular distribution of the positrons at the production target:**
  - **e+ spectrometer collection & transport efficiency**
  - **background rejection issues**
- **huge angular distribution of the re-converted photons**
  - **detected signal includes large fraction of Compton scattered photons**
  - **requires extensive simulations to determine the effective Analyzing Power** A_{e+}

formal procedure:

$$P_{e+} = \frac{\delta}{P_{e-} A_{e+}}$$

ATF experimental layout

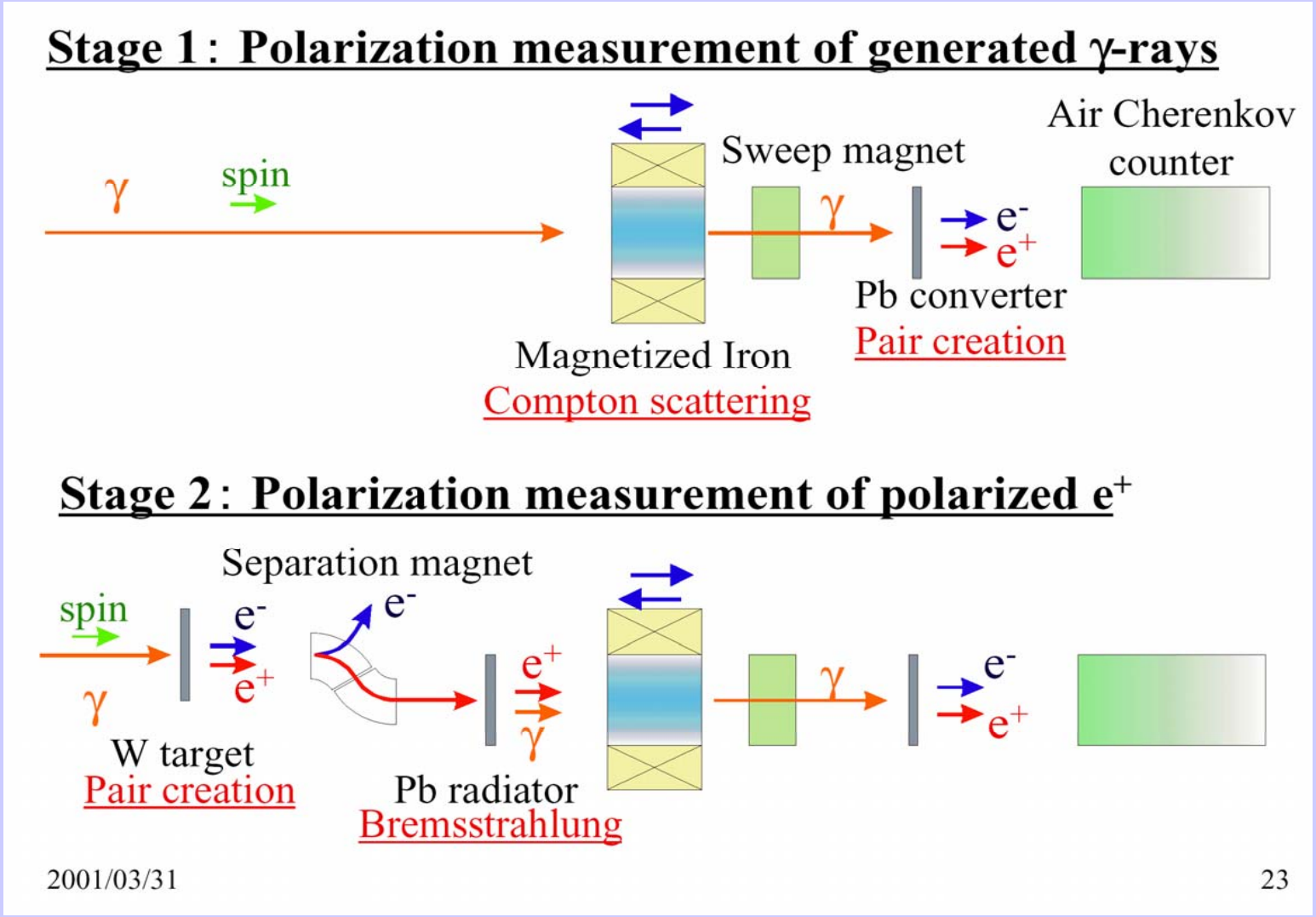

E166: Positron Transport System

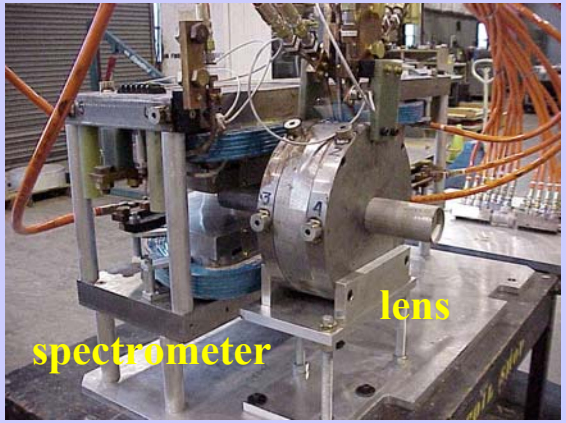

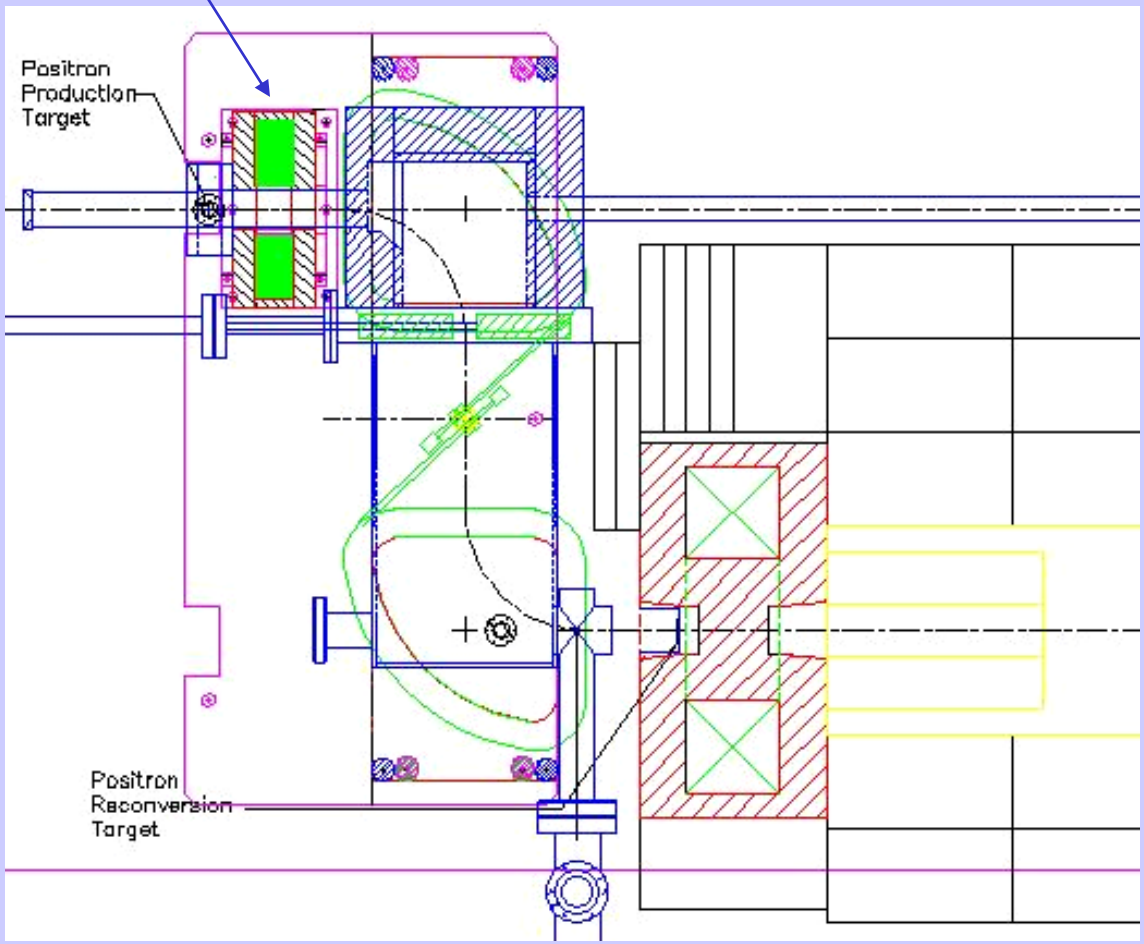

E166 Positron Beam Simulation

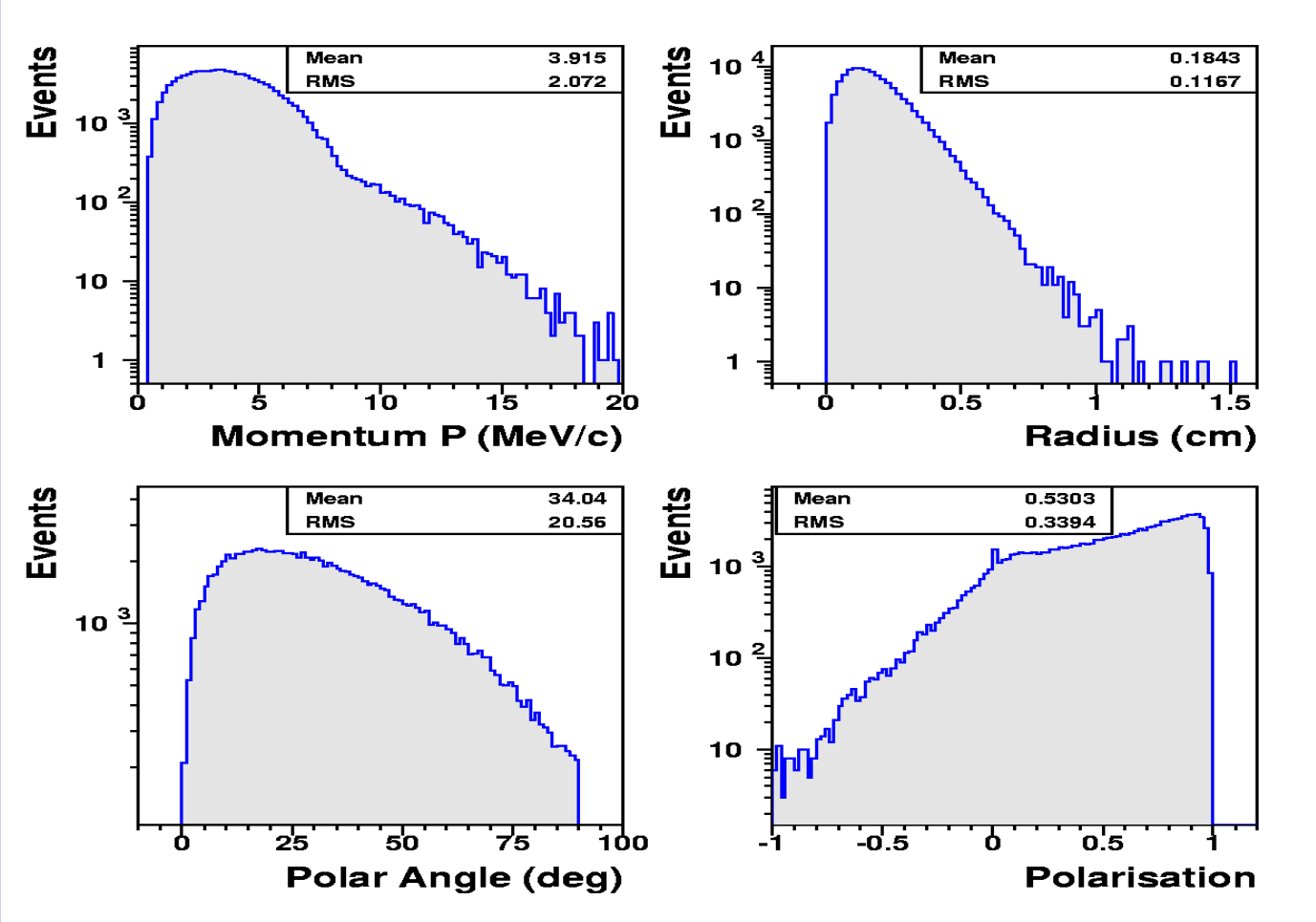

distributions behind the converter target (0.5 r.l. Ti)

(actually we used mainly 0.2 r.l. W)

Positron Transport System

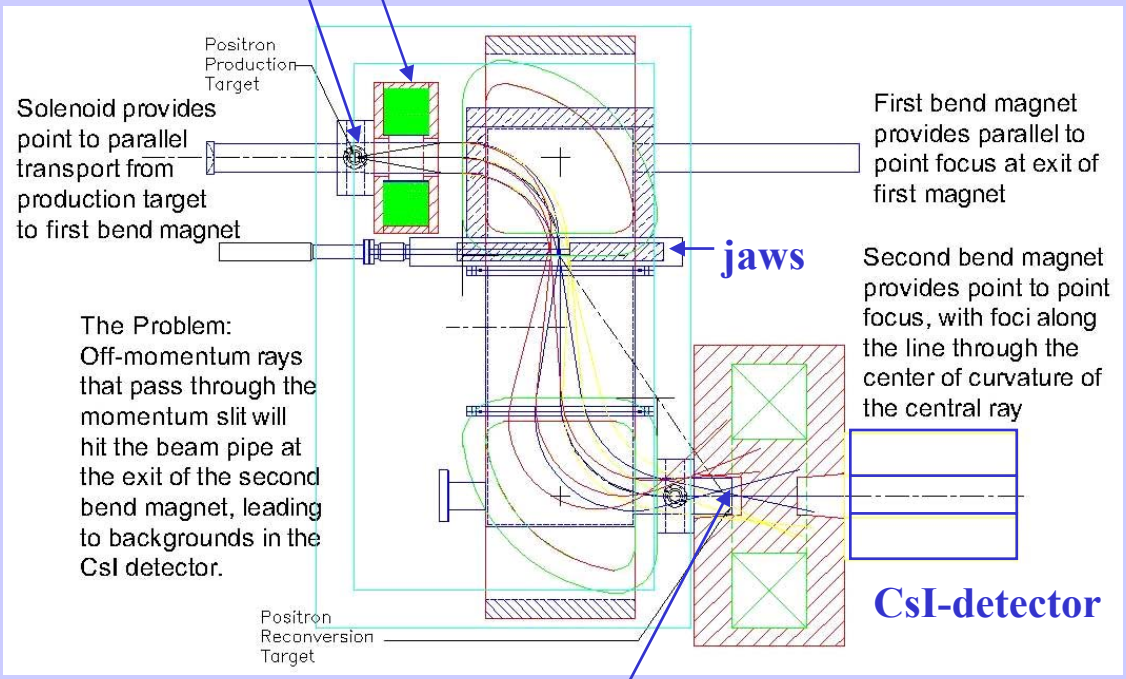

(e- not shown)

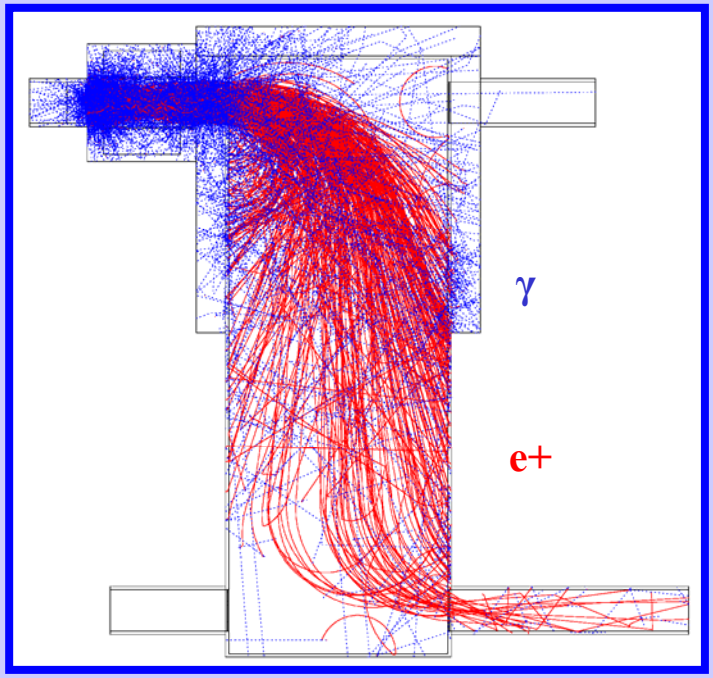

Analyzer Magnet

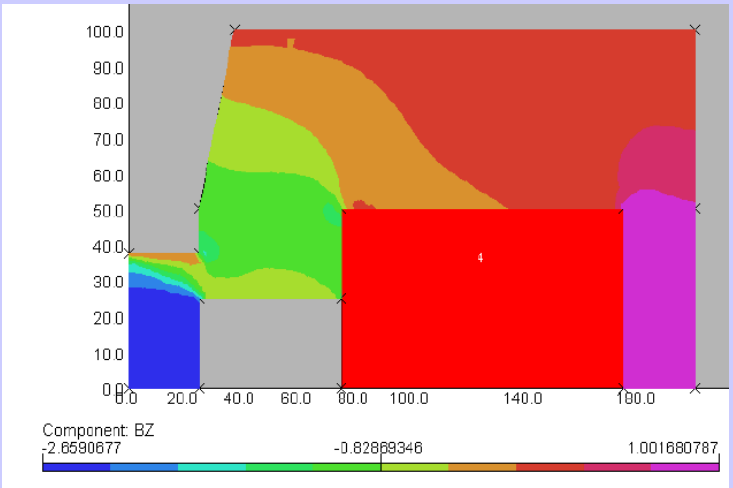

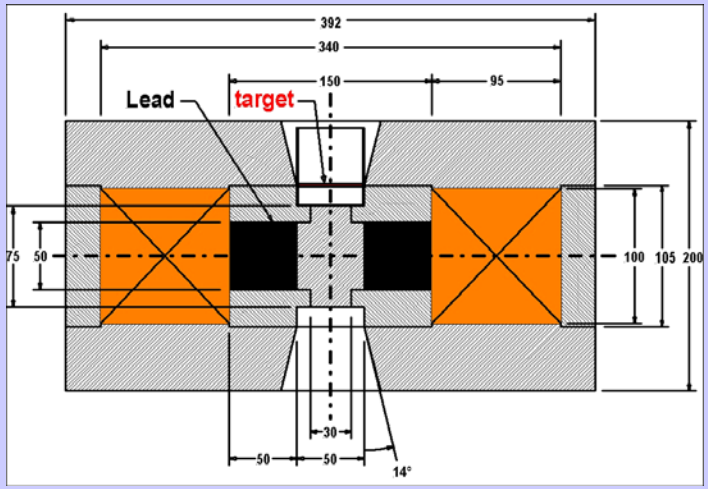

$$P_e = 2 \cdot \frac{g' - 1}{g'} \cdot \frac{M}{n\,\mu_B}$$

g‘ = 1.919 ± 0.002 for pure iron Scott (1962)

Error in e- polarization is dominated by knowledge in effective magnetization M along the photon trajectory:

$$P_e \approx 0.07$$
$$\Delta P_e / P_e < 0.05$$

	active volume
Photon Analyzer:	**50 mm dia. x 150 mm long**
Positron Analyzer:	**50 mm dia. x 75 mm long**

Analyzer Magnet

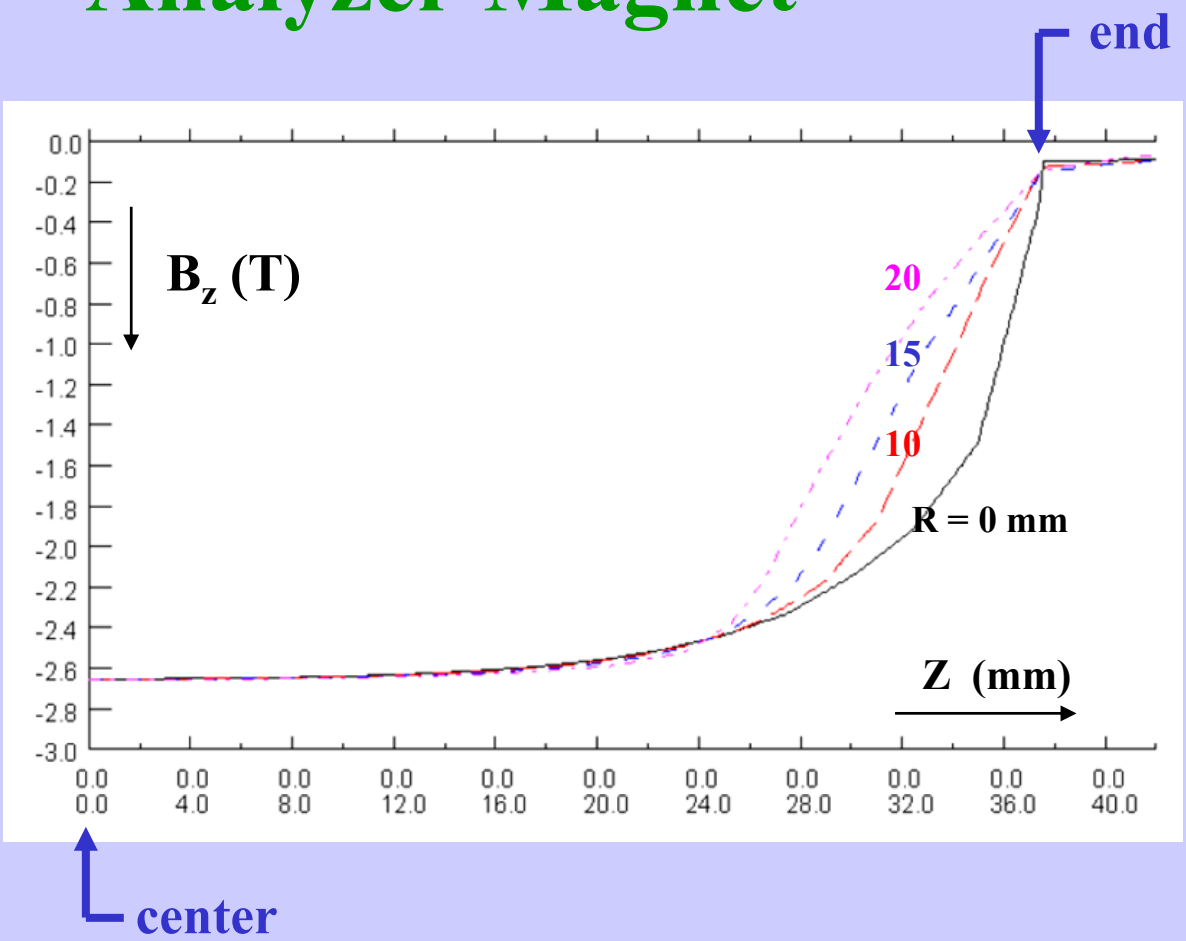

longitudinal field distribution: B_z (R,Z)

from magnetic analysis (Vector Fields OPERA-2d)

field drops gradually towards the ends

Analyzer Magnet

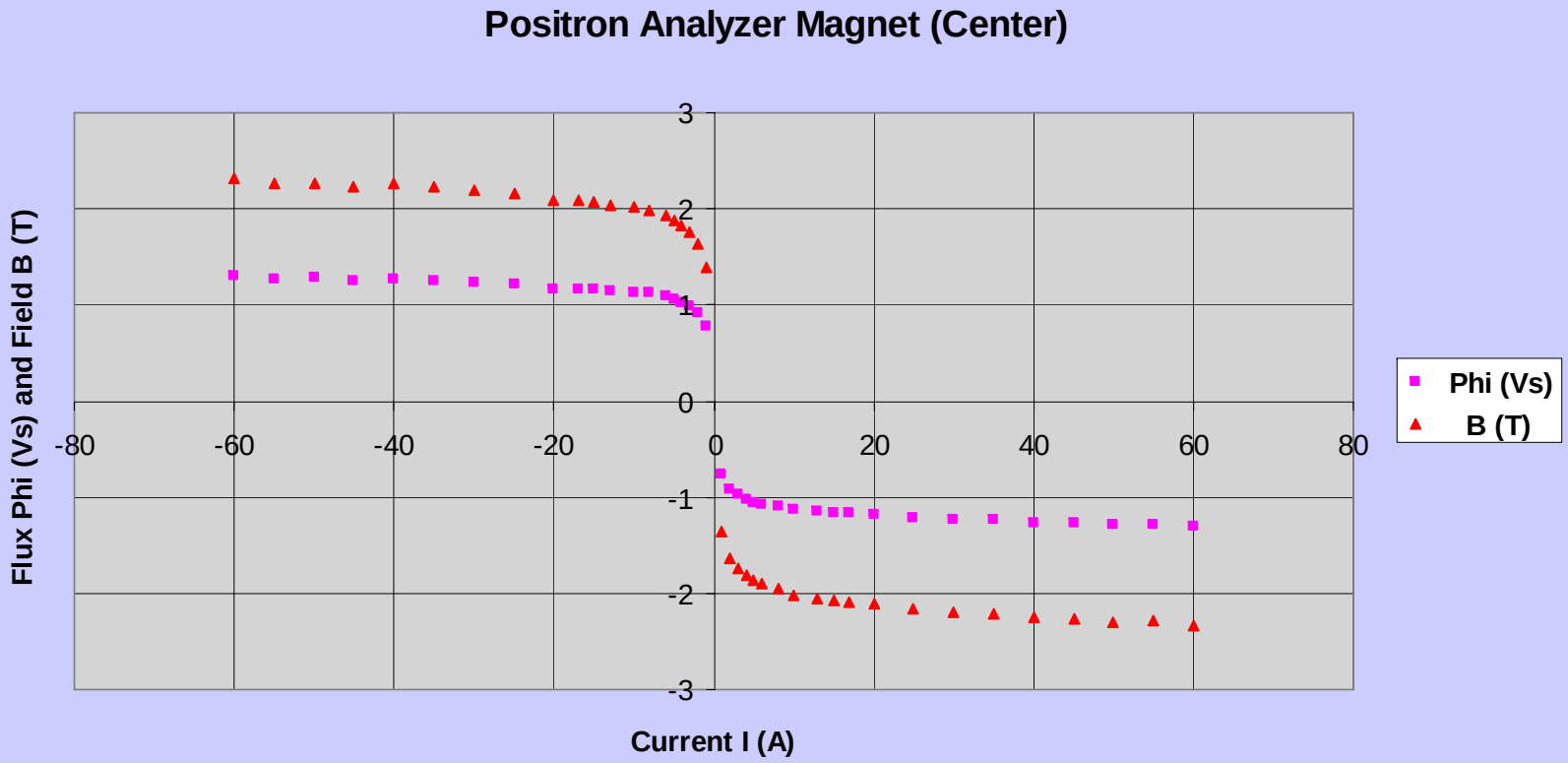

flux and field measurements

Note: polarimetry was always done at full saturation over the central region (±60A)

Analyzer Magnet

electron polarization of the iron (preliminary) : (6.94 ± 0.17) %

$$P_e = \frac{M_S}{\rho_e \mu_b} = \frac{M_S}{M} \frac{M}{\rho_e \mu_b} = 2 \frac{g'-1}{g'} \frac{M}{\rho_e \mu_b}$$

$$\frac{M_S}{M} = 2 \frac{g'-1}{g'} = 0.958 \pm 0.002$$

with $g' = 1.919 \pm 0.002$ for pure iron (Scott 1962)

$$\rho_e = N_{Av} \rho Z / A = 2.206 \cdot 10^{30} / m^3$$

$$\mu_b = \frac{e \hbar}{2 m_e} = 9.272 \cdot 10^{-24} \; Joule / Tesla$$

$$\mu_0 = 4 \pi \cdot 10^{-7} \; T \cdot m / A$$

$$M = (B - B_0) / \mu_0 \qquad B^{max} = \frac{\Delta\Phi}{2 n R^2 \pi} = \frac{1.385 \; Vs}{0.5912 \; m^2} = 2.343 \pm 0.016 \; Tesla$$

$$B_0^{max} = 0.100 \; Tesla \quad (Z = 0; \pm 60 \text{ A})$$

$$M^{max} = 1.785 \cdot 10^6 \; A / m$$

$$P_e^{max} = 2 \frac{g'-1}{g'} \frac{M^{max}}{\rho_e \mu_b} = \frac{0.958 \cdot 1.785 \cdot 10^6}{2.206 \cdot 10^{30} \cdot 9.272 \cdot 10^{-24}} = 0.0836 \pm 0.0006$$

Effective length L_{eff} is shorter than physical length L = 75 mm : $L_{eff} / L \approx 0.83 \pm 0.02$

R (mm)	0	5	10	15	20	25
L_{eff} (mm)	66	65	64	62	60	58
L_{eff} / L	0.88	0.87	0.85	0.83	0.80	0.77

$$\langle P_e \rangle^{eff} = \frac{L_{eff}}{L} P_e^{max} = 0.83 \cdot 0.0836 = 0.0694 \pm 0.0017$$

Analyzer Magnet

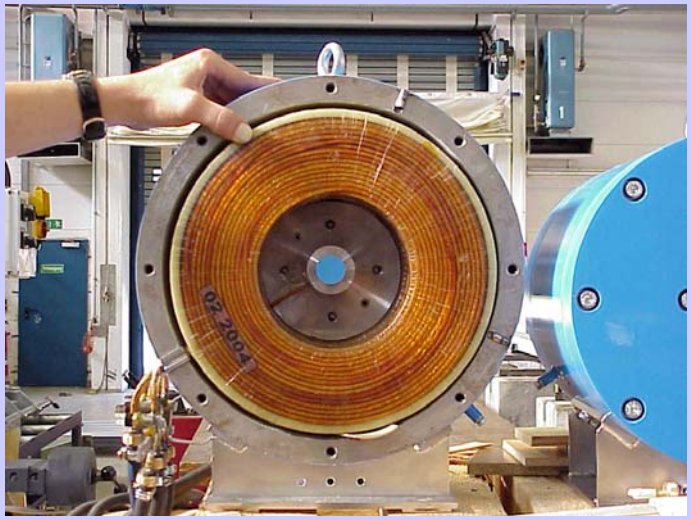

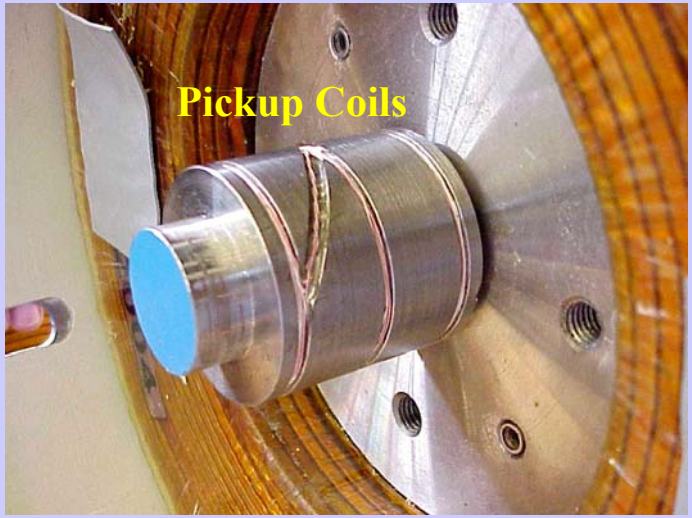

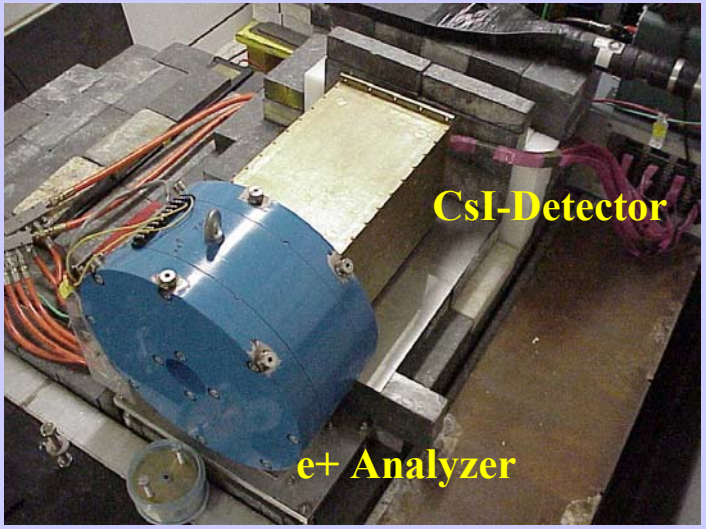

CsI Calorimeter Detector

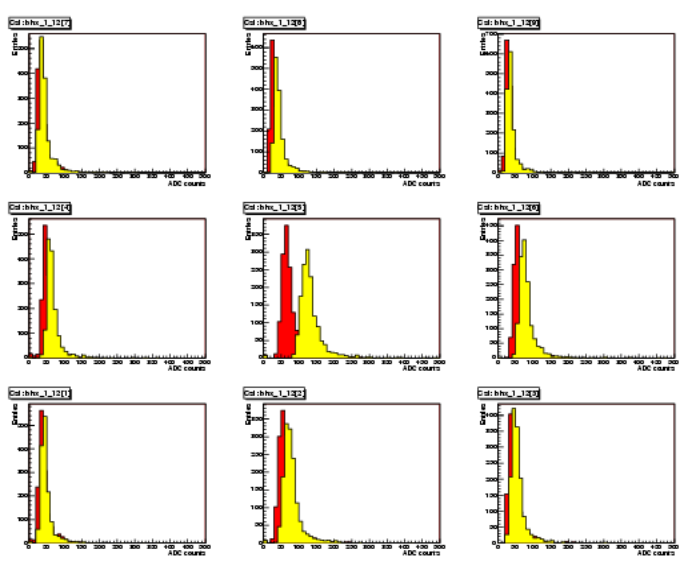

Crystals:	**from Kharkov**
Number of crystals:	**3 x 3 = 9**
Cross section (each crystal):	**6 cm x 6 cm**
Length:	**28 cm**
Density:	**4.53 g/cm³**
Rad. Length	**8.39 g/cm² = 1.85 cm**
Mean free path (5 MeV):	**27.6 g/cm² = 6.1 cm**
No. of interaction lengths (5 MeV):	**4.92**
Long. Leakage (at 5 MeV):	**0.73 %**
Photodiode Readout (2 per crystal): with preamps	**Hamamatsu S2744-08**

Detector Shielding

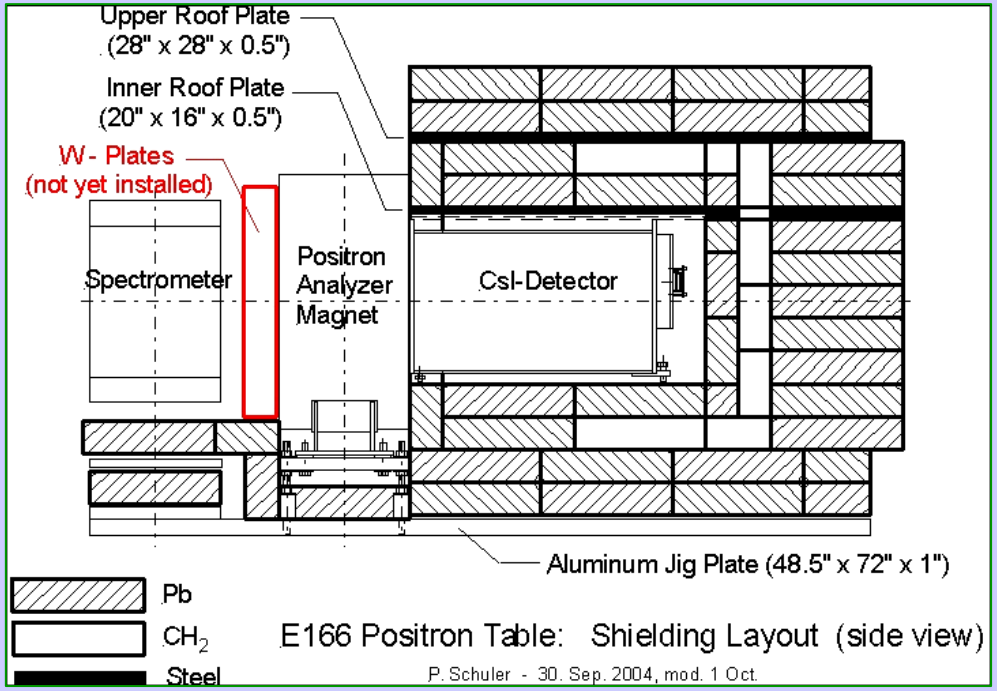

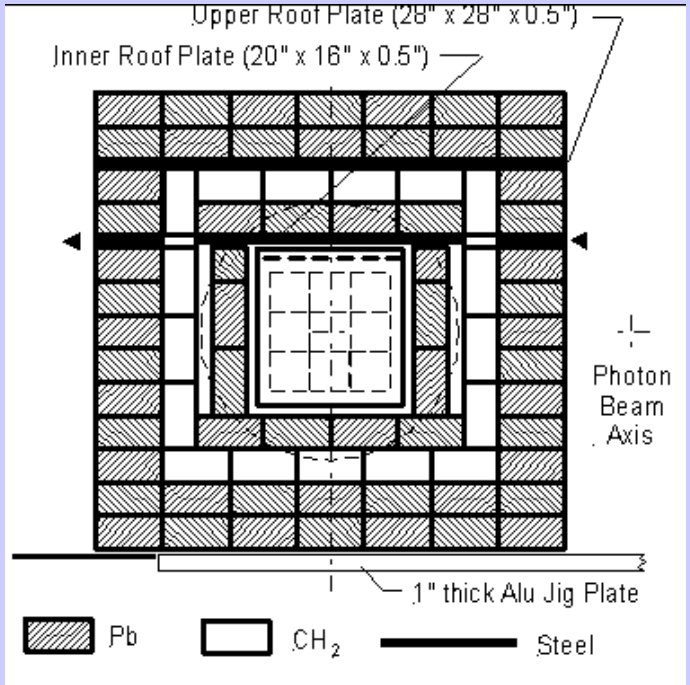

more than 10 tons of lead (1000 bricks) + some tungsten
and yet: plenty of background!

FFTB Tunnel at SLAC

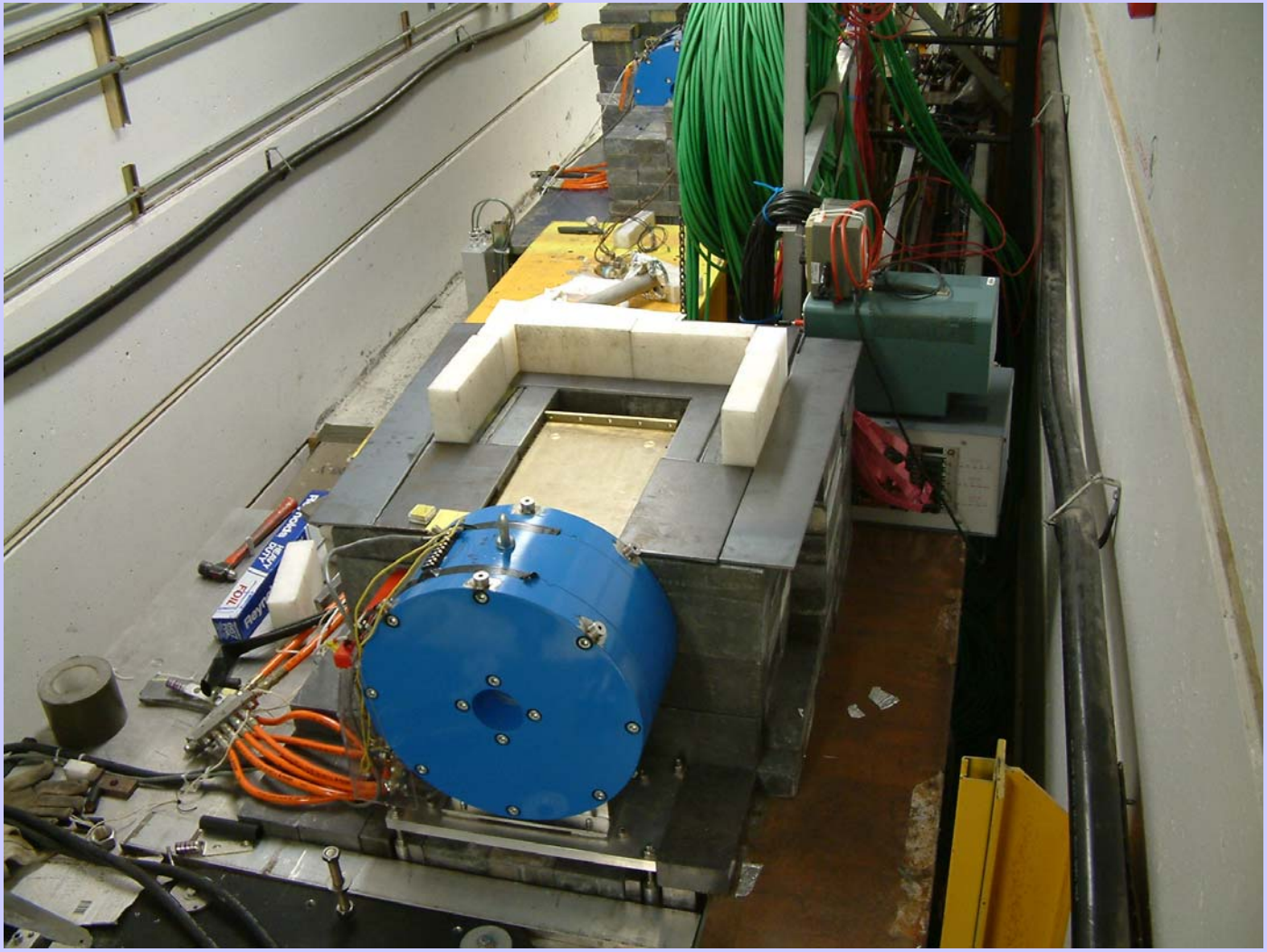

Spin-Dependent Compton Scattering

(employed in Monte Carlo simulation)

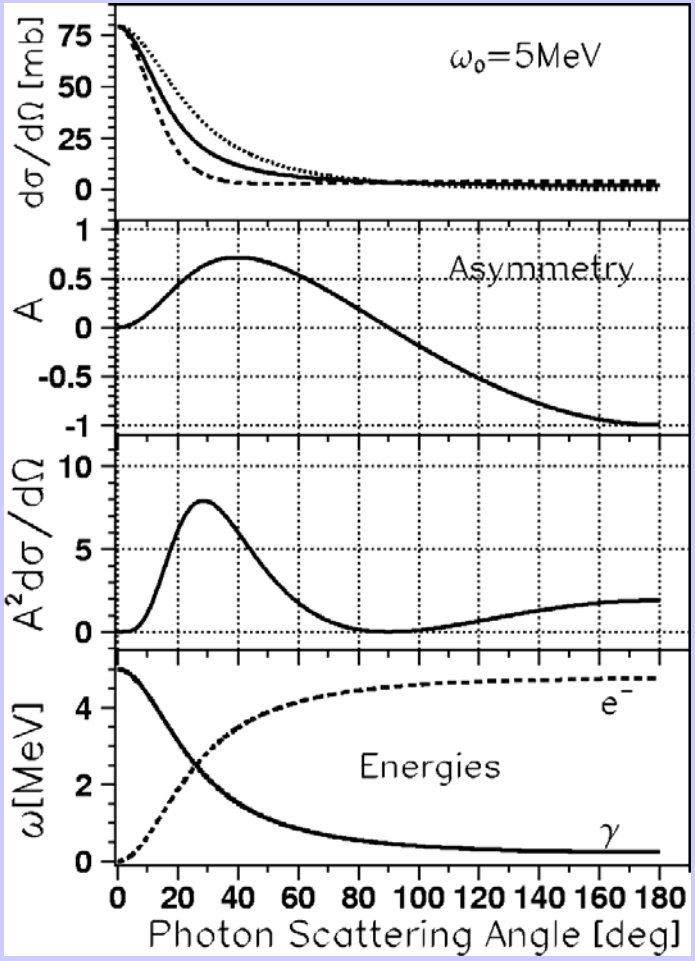

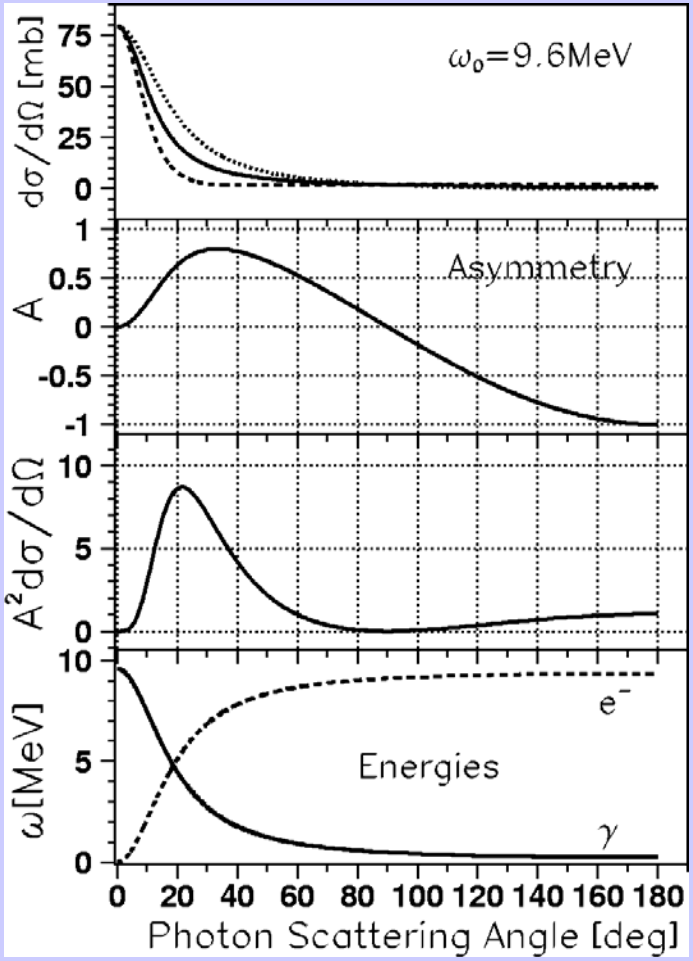

E166 Proposal:

Simulation based on modified GEANT3 code:
for 50 GeV beam energy and hypothetical exp. setup

V. Gharibyan (2003)

layout 4b

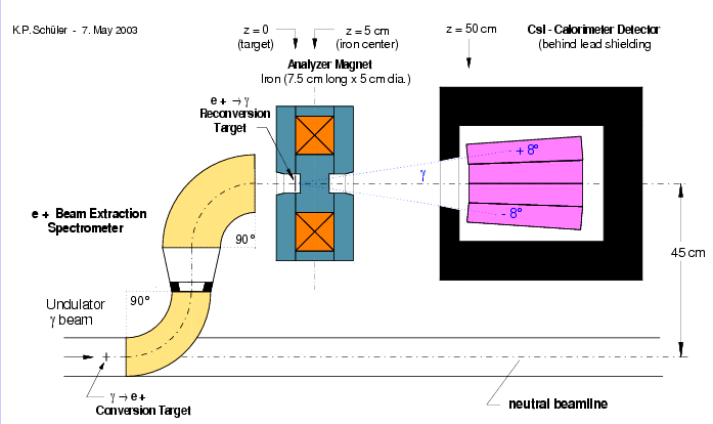

photon spectrum & angulardistribution

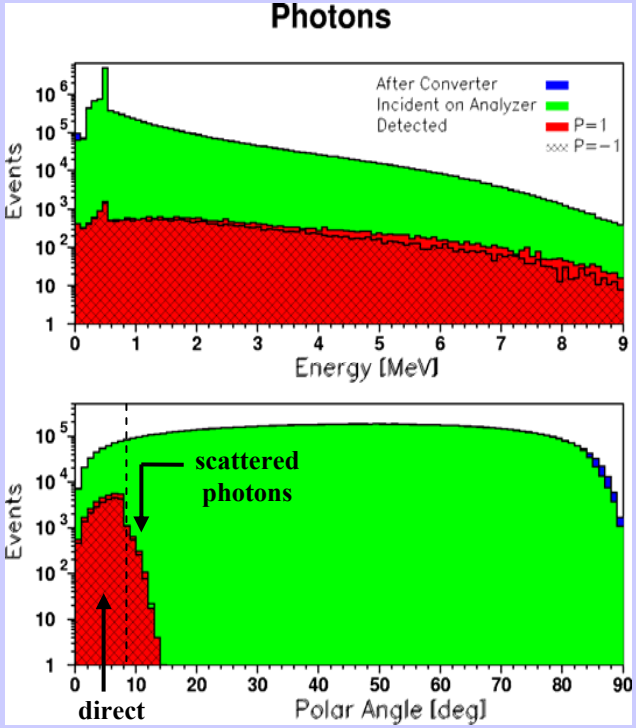

energy-weighted signals & analyzing power vs. energy

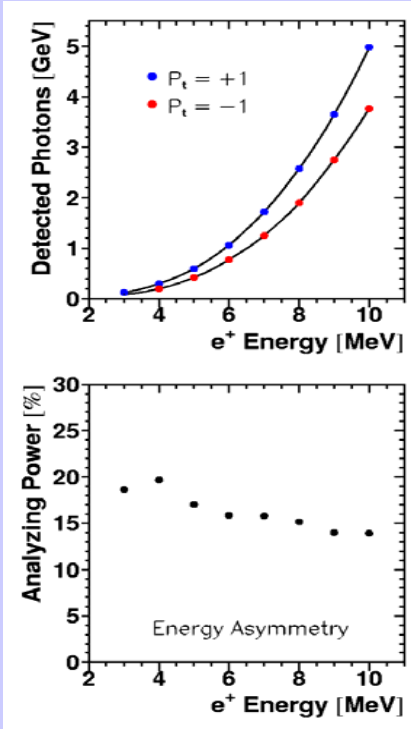

10 Million simulated e+ per point & polarity on the re-conversion target

expected and measured e+ asymmetries

Positron Energy (MeV)	Positron Pol. P_{e^+} (%)	Positron Transport Eff. ϵ_{e^+} (%)	Photon Transport Eff. ϵ_γ (%)	Photon Asym. δ (%)	Analyzing Power A_{e^+} (%)	N_γ in 15 min	15 min Abs.Error ΔP_{e^+} (%)
3	42	1.5	0.045	0.55	18.6	3.7×10^6	4.0
4	61	1.9	0.078	0.84	19.7	8.0×10^6	2.6
5	69	2.1	0.12	0.82	17.0	1.45×10^7	2.2
6	78	2.3	0.20	0.87	15.9	2.44×10^7	1.8
7	84	1.7	0.28	0.93	15.8	2.59×10^7	1.6
8	77	0.9	0.38	0.82	15.0	1.86×10^7	2.2
9	64	0.4	0.50	0.63	14.0	1.09×10^7	3.1
10	68	0.3	0.64	0.66	13.9	1.04×10^7	3.2

E166 Proposal – Table 13

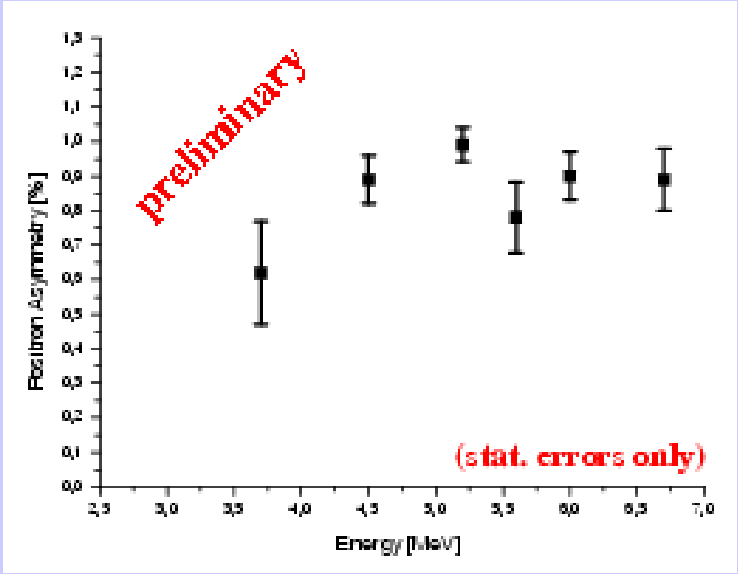

E166 Measurements

actual conditions were different in several ways:

- **beam energy: 50 → 46.6 GeV**
- **beam current: $1 \times 10^{10} \rightarrow 0.5 \times 10^{10}$**
- **lens/spectrometer**
- **CsI-detector geometry**
- **background!!!**

data taking per point req'd not several min's but several days!

also, need new simulation of analyzing power!

Summary on Low-Energy Polarimetry

- **transmission polarimetry has been quite successful both at AFT and in E166 at SLAC**
- **measured E166 positron asymmetries agree well with general expectations**
- **final evaluation of analyzing power and beam polarization is still to be done for E166 data**

High-Energy Compton Polarimetry for ILC

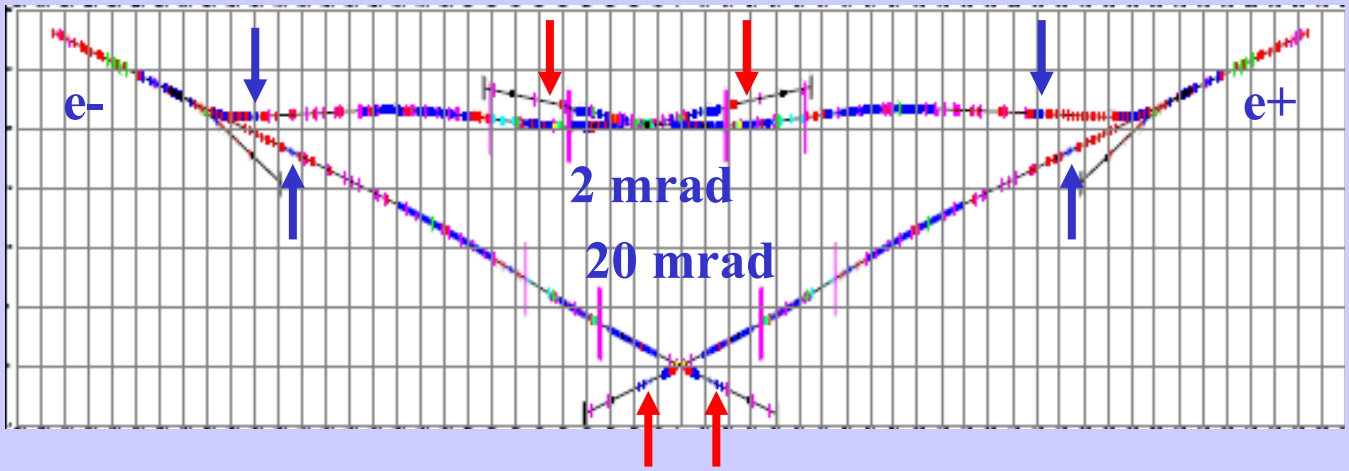

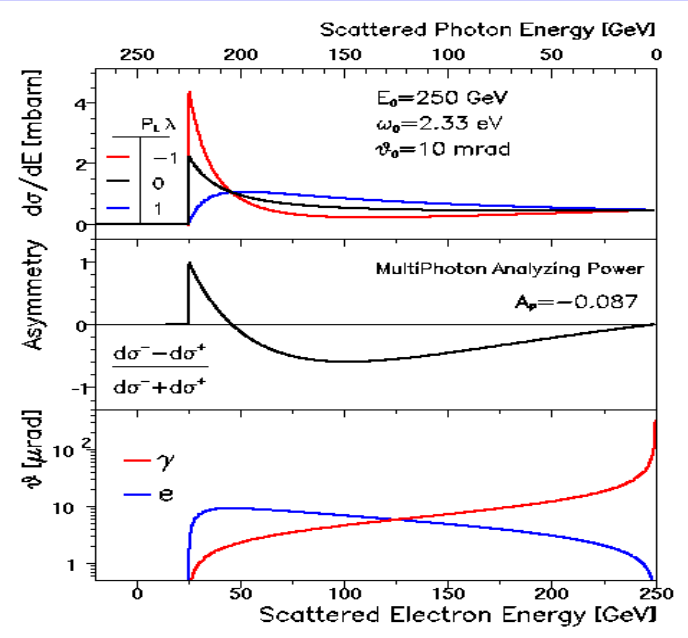

8 polarimeter locations:

- **2 IR's (20mrad & 2mrad)**
- **2 beamlines per IR**
- **2 locations per beamline (upstream & downstream)**

laser choices & parameters

1. Q-switched Nd:YAG laser

pro ⇒ very high pulse energy (up to several 100 mJ),
robust commercial systems, relatively low cost

con ⇒ very low rep-rate (~5 Hz), i.e. only a small sampling fraction (1/2820)
of all ILC bunches can be measured;
inefficient due to long pulse length (ns‘s)

2. TESLA TTF rf-gun type Nd:YLF laser

pro ⇒ pulse pattern matched to ILC bunch & pulse structure;
100% of all ILC bunches will be measured;
high efficiency due to short pulse length (10 ps);
sufficient pulse energy (10-100 μJ) to achieve negligible stat. errors in 1 sec !

con ⇒ non-commercial system, ~ 400 k€ per laser

3. Pulsed Fabry-Perot Cavity (R&D project at Orsay)

pro ⇒ aims for similar performance as (2)

con ⇒ must operate complex laser system remotely in ILC tunnel (reliability!);
feasibility must still be demonstrated (note: HERA Fabry-Perot is not pulsed!)

Laser for TTF injector gun

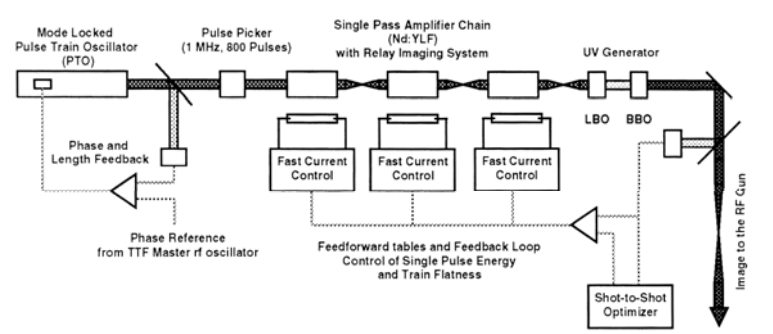

Fig. 1. Schematic overview of the TTF photoinjector laser system.

regen. multi-stage Nd:YLF ampl.
(built by Max-Born-Inst.)
operates at nominal pulse &
bunch pattern of TESLA

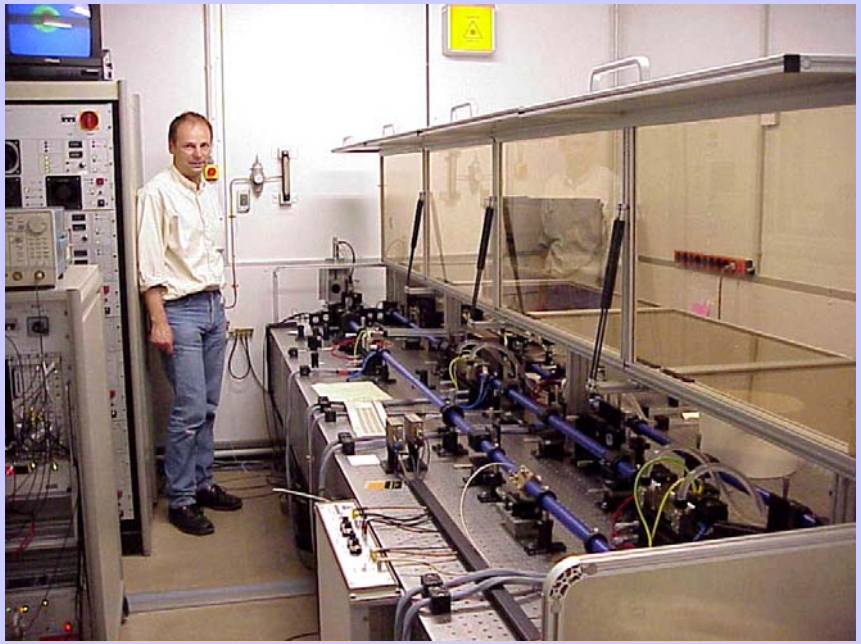

S. Schreiber et al.
NIM A 445 (2000) 427

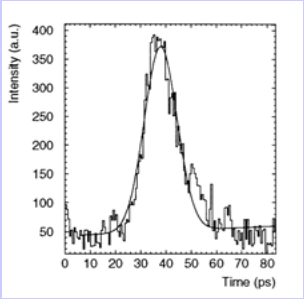

$$\sigma_t = 8 \text{ ps}$$

Tesla design

V. Gharibyan, N. Meyners, K.P. Schüler,
www.desy.de/~lcnotes/notes.html, LC-DET-2001-047

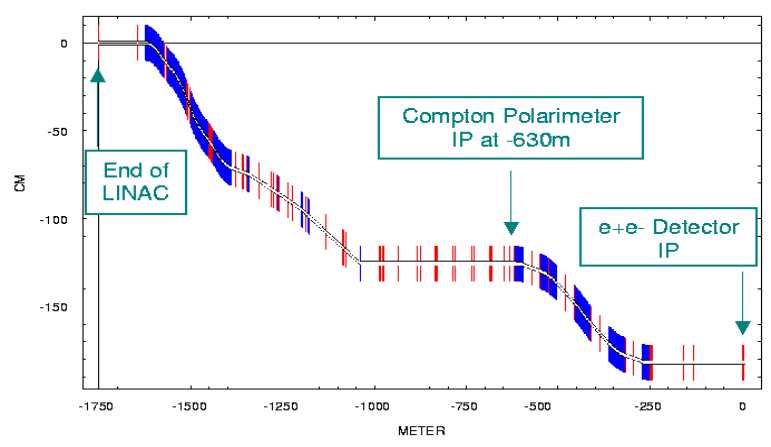

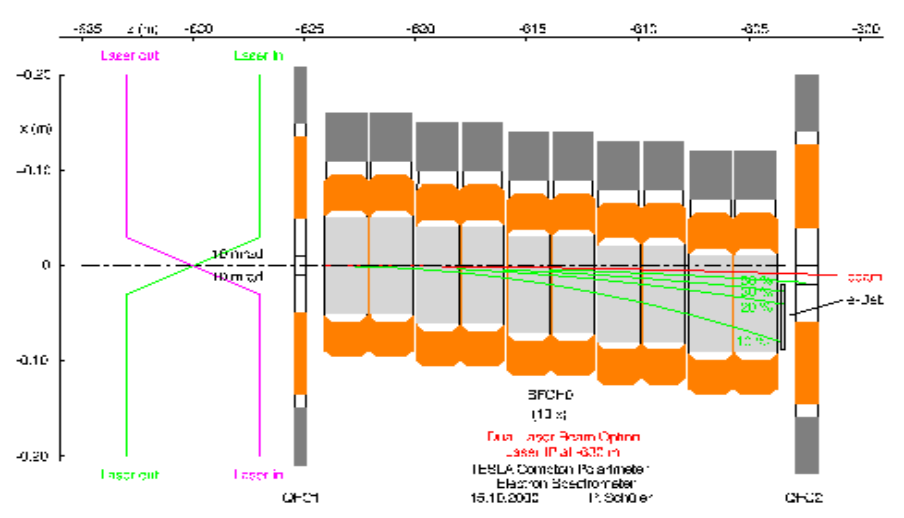

	e^+/e^- beam	laser beam
energy	250 GeV	2.3 eV
charge or energy/bunch	$2 \cdot 10^{10}$	35 μJ
bunches/sec	14100	14100
bunch length σ_t	1.3 ps	10 ps
average current(power)	45 μA	0.5 W
$\sigma_x \cdot \sigma_y$ (μm)	$10 \cdot 1$	$50 \cdot 50$
beam crossing angle	10 mrad	
luminosity	$1.5 \cdot 10^{32} cm^{-2} s^{-1}$	
cross section	$0.136 \cdot 10^{-24} cm^2$	
detected events/sec	$1.0 \cdot 10^7$	
detected events/bunch	$0.7 \cdot 10^3$	
$\Delta P/P$ stat. error/sec	negligible	
$\Delta P/P$ syst. error	$\sim 0.5\%$	

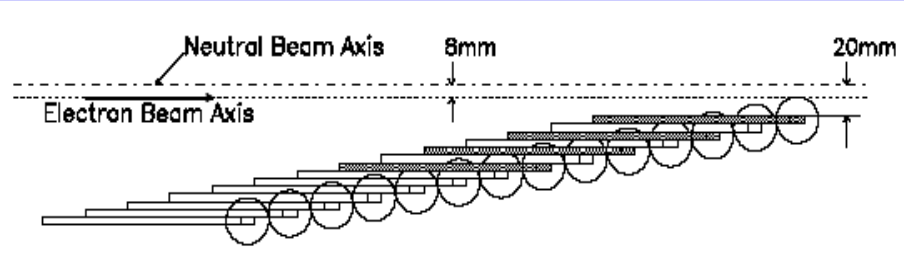

- **minimal space & no special magnets**
- **need to change laser wavelength to UV for Z-pole running**

Chicane Design

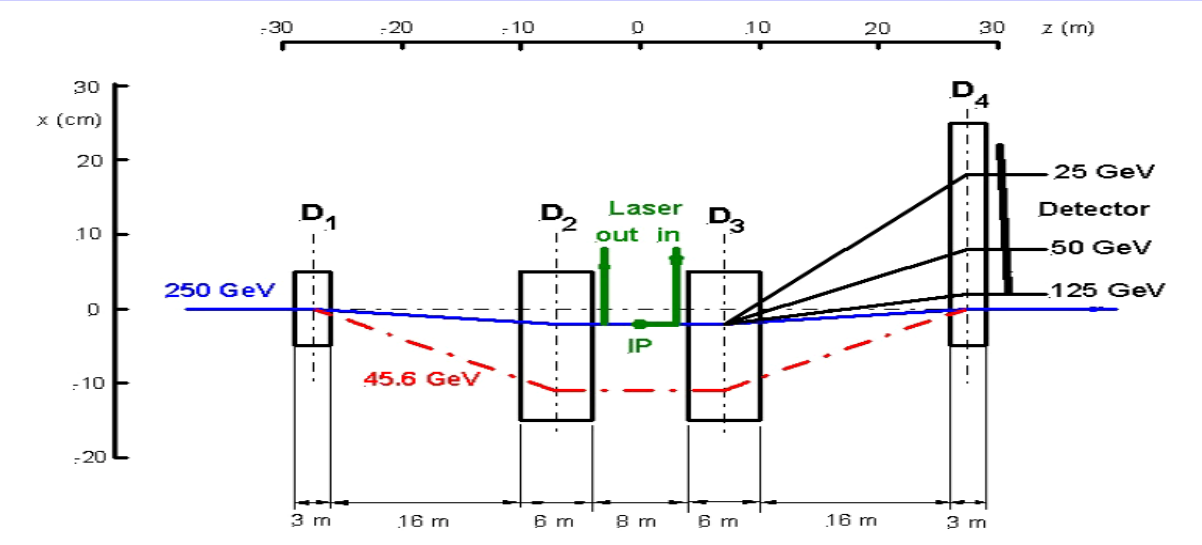

- essential for downstream polarimetry (separates Compton electrons from low-energy disrupted beam background), but adventageous also for upstream polarimetry
- requires ~ 60 meters length
- constant field settings $\int B\, dl$ over wide range of energies
- good acceptance of Compton spectrum at all energies without changing laser wavelength
- laser crossing (Compton IP) at mid-chicane

some technical details

movable laser beam

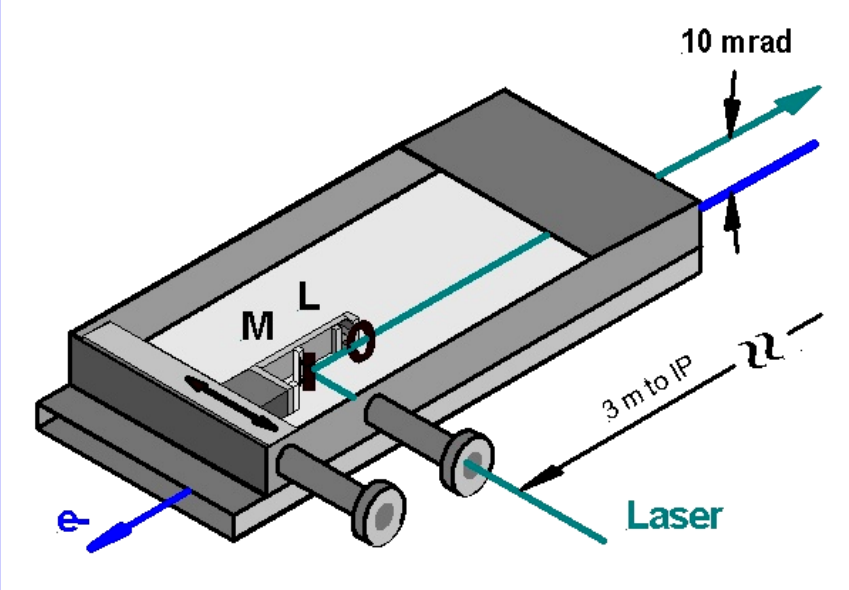

detector hodoscope

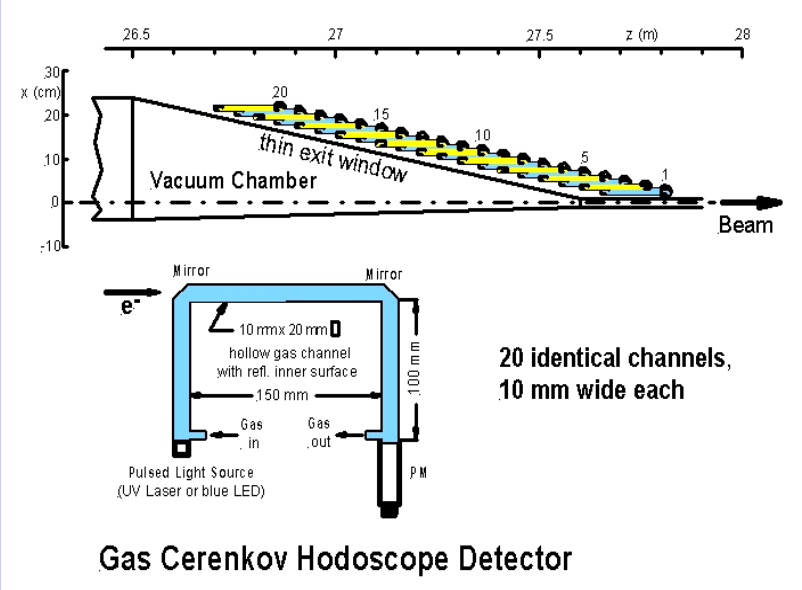

some simulation results

input parameters

0.5 x 10^6	no. of Compton evt's per polarity	
676749.	random seed	
2.33	laser photon energy	(eV)
250.	electron energy	(GeV)
10.	crossing angle	(mrad)
1.50	luminosity	(10^32 / cm² / sec)
0.250	chicane transv. mom. kick	(GeV/c)
2.	magnet length	(m)
20.	cntr. dist. magnets 1&2 (3&4)	(m)
10.	cntr. distance magnets 2&3	(m)
0.7	dist. mag. 4 edge to det. ch. n	(m)
20	no. of det. channels (max. 100)	
10.	det. channel x-size (hor.)	(mm)
20.	det. channel y-size (vert.)	(mm)
150.	det. channel length along z	(mm)
20.	distance det. ch. 1 to beam	(mm)
50.	z-dist. btw. det. channels	(mm)
1.	meas. time for stat. error	(sec)
0.80	beam pol. to calculate stat. error	

E_0 = 250 GeV

ω_0 = 2.33 eV (green laser)

L = 1.5 x 10^{32}/cm²/sec

results

Ch. #	x [mm]	N+	N-	A	Rate*A²	Rate [MHz]	dP/P [%]
1	25	60,682	23,368	-0.444	0.337	1.710	0.228
2	35	45,868	17,348	-0.451	0.262	1.287	0.260
3	45	35,673	16,012	-0.380	0.152	1.052	0.335
4	55	28,337	16,029	-0.277	0.069	0.903	0.486
5	65	22,996	16,956	-0.151	0.019	0.813	0.924
6	75	18,333	17,876	-0.013	0.000	0.737	11.521
7	85	15,248	18,744	0.103	0.007	0.692	1.466
8	95	12,025	19.818	0.245	0.039	0.648	0.646
9	105	9,881	20,480	0.349	0.075	0.618	0.473
10	115	7,815	21,525	0.467	0.130	0.597	0.370
11	125	6,246	21,961	0.557	0.178	0.574	0.324
12	135	4,849	22,795	0.649	0.237	0.562	0.289
13	145	3,479	23,315	0.740	0.299	0.545	0.266
14	155	2,385	23,821	0.818	0.357	0.533	0.250
15	165	1,346	24,171	0.895	0.416	0.519	0.238
16	175	457	20,900	0.957	0.398	0.435	0.249
17	185	0	0				
18	195	0	0				
19	205	0	0				
20	215	0	0				

overall stat. error: dP/P = 0.082%

for dT = 1 sec (very fast!)

syst. errors: ~ 0.25%

Summary on High-Energy Polarimetry

- **detailed designs are being worked out at SLAC and DESY**
- **chicane configuration has been adopted for all locations (upsteam & downstream)**
- **different laser choices still being explored**
- **expect ultimate systematic error of dP/P ~ 0.25%**